Ac transport studies in polymers by a resistor network and transfer matrix approaches: application to polyaniline.

H.N. Nagashima,* R. N. Onody†and R. M. Faria‡

Instituto de Física de São Carlos

Universidade de São Paulo - Caixa Postal 369

13560-970 - São Carlos, São Paulo, Brasil.

Abstract

A statistical model of resistor network is proposed to describe a polymer structure and to simulate the real and imaginary components of its ac resistivity. It takes into account the polydispersiveness of the material as well as intrachain and interchain charge transport processes. By the application of a transfer matrix technique, it reproduces ac resistivity measurements carried out with polyaniline films in different doping degrees and at different temperatures. Our results indicate that interchain processes govern the resistivity behavior in the low frequency region while, for higher frequencies, intrachain mechanisms are dominant.

PACS numbers: 72.80.Le; 05.60.+w; 84.37.+q

---

*haroldon@ifsc.sc.usp.br

†onody@ifsc.sc.usp.br

‡faria@ifsc.sc.usp.br

1 Introduction

The strong variation of electrical conductivity of conjugated polymer films resulting from chemical doping, as seen in the insulator-to-metal transitions, was first observed in polyacetylene [1]. Since then, a great amount of experimental and theoretical studies has been done to elucidate the mechanisms involved in the electronic transport phenomena. Initial efforts were dedicated to understand the conduction mechanism along a single chain, with the SSH model [2], a theoretical one-electron framework based on the Hückel approach, which most successfully described the one-dimensional trans-polyacetylene. Doping mechanisms associated with chain defects brought into vogue the concepts of solitons and polarons as intermediate levels in the electronic structures of a single conjugated polymeric chain [3]. The number of such excitonic defects are directly related with the doping level: from weak to moderate doping the conduction mechanism is mainly due to electronic hopping, while extended states are reached by strongly doped samples. In macroscopic samples, for which extremely large conductivity changes can be observed (circa of 15 orders of magnitude), interchain processes must be taken into account owing to interactions brought about by the molecular packing. Theoretically, such interactions may be represented by the interchain exchange integral, which contribute significantly to the final conductivity value.

The major difficulty in the study of bulk conductivity of polymeric materials lies in their highly disordered structure. The carrier transport should contain

competing intrachain and interchain processes, and the challenge is not only to identify the contribution of each process, but also to quantify them. In this context, the alternating conductivity technique is an appropriate tool due to its spectroscopic character.

Among other theoretical treatments, statistical models have also been applied to describe polymerization processes [4], as well as, to study electrical properties of polymers [5, 6]. These models are essentially based on percolation concepts and have the advantage of simultaneously treating the phenomena involved on both a microscopic and a macroscopic scale. Baughman and Shacklette proposed a random resistor network model which successfully explained the conductivity dependence on the conjugated length [5]. Andrade et al [6] investigated the influence of percolation disorder on the electrical behavior in the dc regime. The distinction between intrachain and interchain mechanisms, both equally important to bulk conductivity, nevertheless requires a more detailed analysis.

In this paper we investigate the conductivity properties of weakly doped polyaniline in the presence of an alternating electric field, from both the theoretical and experimental perspectives. Ac conductivity measurements were carried out in polyaniline (PANI) films at different temperatures and doping degrees. The system is theoretically described by a percolation model where the basic ingredients responsible for the conductivity are incorporated. The model also takes into account the polydispersiveness of the material, the interchain and

3

the intrachain charge transport. The real and imaginary parts of the resistivity were determined using a transfer matrix technique. At low frequencies, interchain processes are more important and dominate the transport mechanism. On the other hand, at high frequencies charge transport should be restricted along the polymer chains, so intrachain processes should be dominant. Both regimes are well described by our model, which also reproduces the experimental results in a remarkable way.

2   Theoretical Model and Numerical Simulations

The theoretical model introduced in this paper allow us to focus two important aspects of the material: its geometrical structure and its electrical conductivity.

First, we build a strip by juxtaposing N square cells, each cell with L x L sites (see Fig.1). Here, cells are used to conciliate the polymer size distribution, obtained experimentally by the Gel Permeation Chromatography method, with the transfer matrix technique developed by Derrida *et al.* [7]. The use of cells was applied here to calculate the electrical conductivity *without* excceeding the capacity of the computer's memory. In its original formulation [7], the tranfer matrix acts on a random and *ramified* structure of resistors. Here, however, only a non ramified structure is possible. Therefore, we construct a cell which contains only linear structures with a Gaussian size distribution and fixed density. The information of one cell is stored and transferred, by the matrix method, to the next cell.

An empty lattice site i of the cell is randomly occupied, representing the presence of a monomer. We shall call this site the *growing tip*. The chain size l is taken from a *Gaussian* distribution probability centered in l_0 with dispersion Δl. An *empty* site j, nearest neighbor of the growing tip i, is randomly occupied and a resistance R_c is attributed to the bond connecting these two monomers (sites). The site j becomes now the new growing tip. The process is repeated until the chosen polymer size is reached. If the polymer cannot reach the specified length, it is discarded. Clearly, a self-avoiding scheme is used to mimic the excluded volume interaction.

After the chain has reached the selected size, a search in all of its monomers is performed looking for a pair of nearest neighbor monomers (which can belong or not to the same chain), not connected by R_c. If such a pair is found then these monomers are connected, with probability p_d, by a RC circuit. This RC circuit is a parallel association where C is the capacitance and R_i is the interchain resistance . The idea is to incorporate induced charges and hopping (or tunneling) mechanisms. As we shall see, p_d is related to the doping level and we call it the doping parameter.

Repetition of the procedure described above built new polymer chains inside the cell until some concentration k of the occupied lattice bonds is reached. Let N_{ob} be the number of occupied lattice bonds, i. e., N_{ob} = number of resistances R_c + number of impedances Z (the equivalent impedance of the circuit RC) and N_{eb} the number of empty lattice bonds (corresponding to infinite resistances)

then $k = N_{ob}/(N_{ob} + N_{eb})$. If $k = 0.5$ the system is at the critical bond per-colation threshold of the square lattice. A typical cell is depicted in Fig.1. It is considered that a bias voltage is applied on both sides, being L the distance between the electrodes.

To determine the longitudinal resistivity $\rho_{//}$ of the cell, which is the resistivity in the direction of the current flow, we follow the tranfer matrix method [7]. Compared to the two other main approaches - resolution of Kirchoff's equations and node elimination, this technique has many advantages. It consumes less CPU time, it avoids troubles with dangling bonds or isolated clusters, and the conductivity is calculated exactly. Of course, care should be taken when passing from one cell to another: horizontal and vertical bonds *on the boundary* must be stored in order to correctly construct the next cell. We used around $N \sim 100,000$ cells in our simulations.

Simulated curves $\rho_{//}$ versus f (the frequency of an ac electric field) are presented in Fig.2. They exhibit two plateaus, i. e., two regions in which the resistivity is frequency-independent: one at low frequencies and the other at high frequencies. Between these two plateaus the resistivity decays with the frequency, obeying approximately the relation $\rho_{//} \propto f^{-\alpha}$ with $\alpha = 1.9$. It does not agree with the measured value $\alpha \simeq 1.2$, which is the slope of the experimental curves of Fig. 3. This discrepancy, however, disappears when we consider, as we shall see later, the interchain resistance R_i dependence with the frequency f. Figures 2a, 2b and 2c correspond to simulations performed at concentration

6

$k = 0.5$ and they show, respectively, the influence of p_d, R_c and R_i in the $\rho_{//}(f)$ curves. R_i acts in the low frequency plateau, R_c in the high frequency and p_d causes the whole curve to shift up and down. The interpretation of these parameters will be discussed below, when the simulated results and the experimental curves carried out in PANI films are compared. Figure 2d was obtained at fixed values of p_d, R_c and R_i but for two different concentrations $k = 0.5$ and $k = 0.6$. Increasing k simply displaces the whole curve of resistivity downward in a frequency independent way. This is expected since, to increase the concentration k is equivalent to substitute a number of empty bonds (infinite resistances) by occupied bonds (finite resistances). Note that the effects of increasing k or p_d are very similar - both are frequency independent and decrease the resistivity. As the concentration k does not essentially alter the form of the curves, in the rest of this paper we restrict the simulations to be performed at $k = 0.5$.

3   Experimental Resistivity

Responses to alternating electrical field applied in doped conjugated polymers have been an important subject of research when charge transport phenomena are involved. Some ac results, conductivity versus frequency, have already been reported in the literature, with polyacetylene [8, 9], poly(3-methylthiophene) [10] and poly(o-methoxyaniline) [11]. Here we present some results carried out with polyaniline films for different doping degrees and different temperatures.

Polyaniline is a common name for a family of polymers consisting of a sequence of oxydized [-(C6H4)-N=(C6H4)=N-] and reduced [-(C6H4)-(NH)-(C6H4)-(NH)-] units. Three distinct forms have been identified and the emeraldine form, which contains an equal number of oxydized and reduced segments, has been the most frequently studied. Polyaniline was synthesized and processed as described elsewere [12]. Flexible and free-standing films were obtained. Upon protonation, plunging the emeraldine sample into aqueous HCl solutions of different molarities, its resistivity changes from the characteristic of poorly conducting semiconductors ($\rho \sim 10^{10}$ Ω.cm) to metals ($\rho \sim 10^{-1} - 10^{-3}$ Ω.cm). Circular,12 μm in thick samples, had central gold electrodes of a diameter equal to 0.5 cm evaporated on both sides. Impedance measurements were carried out using a controlled Frequency Response Analyser coupled to a Potentiostat which operates in the 10^{-1} to 10^6 Hz frequency range.

Figure 3 shows measurements of real and imaginary components of ac resistivity of PANI films under conditions: a) doped in HCl solution of $0.1M$ at $300K$ (measurement denoted by M_1); b) doped in HCl of $0.01M$ at $300K$ (M_2); and c) doped in HCl of $0.1M$ at $200K$ (M_3). It should be that the real and imaginary parts of the longitudinal resistivity $\rho_{//}$ are proportional to these measured resistivities [13]. The sample used in the curves of Fig. 3 (b) is less doped than that of Fig. 3 (a), while the sample in Fig. 3 (c) is equally doped but it is obtained at a lower temperature.

4   Results and Discussion

The curves of Fig.3 are faithfully reproduced by our model by fixing R_c and p_d values and having a frequency-dependent interchain resistance R_i as shown in the insets of Fig. 4a. Fig. 4b (M_2 measurement) is obtained with $R_c = 2.0\omega$ and $p_d = 0.18$. Finally for M_3, $R_c = 0.5\omega$ and $p_d = 0.21$ - the same values as in M_1 the differences being on account of the hopping resistance R_i. At low frequencies R_i of M_3 is ten times bigger than that of M_1 (see insets of Fig. 4a and 4c). Then from these results we conclude that: i) the increase in the doping can either be simulated by diminishing R_c or increasing p_d and ii) decreasing the temperature the sample resistance increases, as expected. The resistance R_c represents the conduction mechanism along a single chain. It should depend only slightly on the temperature (see for example the SSH model [2]), but it is sensitive to the doping degree. The doping parameter p_d changes with the doping degree (as can be seen in curves 4(a) and 4(b)), but it is frequency independent. In a highly disordered bulk structure, on the other hand, interchain charge transfer processes of electronic carriers can be represented by a distribution of energy barriers W of interchain hopping (or phonon-assisted tunneling). Since R_i represents, in our model, the interchain processes, its dependence on the frequency is explained in terms of this energy barrier distribution. A given waiting time τ is associated with an energy barrier W by $\tau \sim exp(W/kT)$. In the low frequency region, where $f < \tau^{-1}$, electron motion is hampered mainly by the high energy barriers (high W), which represent interchain obstacles. For

$f > \tau^{-1}$, on the other hand, the electronic carriers become localized in small regions of low energy barriers, being therefore, more mobiles. This description agrees qualitatively with the frequency-variation of R_i shown in the insets of Fig.4. To have a more formal insight on the subject, let us consider the random free-energy barrier model.

This model is an elegant way to approach ac conductivity in polymeric disordered systems. In this formalism all information about disorder is contained in the hopping time distribution function $\psi(t)$. According to J. C. Dyre [14] $\psi(t)$ is determined by hopping over random distributed energy. He used the continuous time random walk and the effective medium approximation to solve the model and to derive a simple expression for the complex conductivity σ as a function of the frequency f

$$\sigma(f) = C[-if + \frac{if \ln(\frac{\gamma_{max}}{\gamma_{min}})}{\ln(\frac{1+if/\gamma_{min}}{1+if/\gamma_{max}})}]$$

where C is a constant depending among other parameters on the density of carriers, γ_{max} and γ_{min} are two parameters related to the jump frequency.

In our model, the R_i dependence with f was determined by adjusting the real and the imaginary parts of the simulated resistivity, for each frequency, to the experimental values. This give us an infinity of fitting parameters. But now we can compare our results with those predicted by Dyre's solution. The advantage is that Dyre's hopping resistance has only three fitting parameters for all frequencies. Figure 5 shows that the adjusted R_i is in reasonable agreement with Dyre's theory.

10

Extrapolating the dependence of R_i with f for *high* frequencies (unattainable in our equipment), as shown in the insets of Fig. 4, our simulations anticipate the emergence of a second plateau for the real component of the resistivity. This prediction is compatible with other results found for a polymeric blend [15].

5   Summary and Conclusions

In conclusion, we introduce a model which carefully takes into account the geometric aspects of the real polymeric structure. It considers the polymer chains being constructed from a Gaussian size distribution and in the presence of the excluded volume interaction. It incorporates, in a simple way, the existence of both intrachain and interchain charge transport mechanisms. Simulations based on a tranfer matrix technique and performed at the critical percolation threshold, reproduces the measured resistivity in PANI films in a large range of frequencies for different doping and temperature conditions. Estimatives of the critical conductivity exponent using a finite size scaling approach will be the object of a forthcoming paper.

6   Acknowledgments

References

[1] C. K. Chinag, C. R. Fincher, Y. W. Park, A. J. Heeger, H. Shirakawa, E. J. Louis, S. C. Gau and A. G. MacDiarmid, Phys. Rev. Lett. **39**, 1098 (1977).

[2] W. P. Su, J. R. Schrieffer and A. J. Heeger, Phys. Rev. B **22**, 209 (1980).

[3] Y. Lu, *Solitons and Polarons in Conducting Polymers* (World Scientific, Singapore, 1988).

[4] L. S. Lucena, J. M. Araújo, D. M. Tavares, R. L. da Silva and C. Tsallis, Phys. Rev. Lett. **72**, 230 (1994).

[5] R. H. Baughman and L. W. Shacklette, J. Chem. Phys. **90**, 7492 (1989).

[6] J. S. Andrade Jr., N. Ito and Y. Shibusa, Phys. Rev. B **54**, 3910 (1996).

[7] B. Derrida, J. G. Zabolitzky, J. Vannimenus and D. Stauffer, J. Stat. Phys. **36**, 31 (1984).

[8] A. J. Epstein, H. Rommelmann, M. Abkowitz and H. W. Gibson, Phys. Rev. Lett. **47**, 1548 (1981).

[9] K. Ito, Y. Tanabe, K. Akagi and H. Shirakawa, Phys. Rev. B **45**, 1246 (1992).

[10] W. Rehwald, H. Kiess and B. Binggeli, Z. Phys. B **68**, 143 (1987).

[11] C. M. Lepienski, R. M. Faria and G. F. Leal Ferreira, Appl. Phys. Lett. **70**, 1906 (1997).

[12] L. H. C. Mattoso, R. M. Faria, L. O. S. Bulhes and A. G. MacDiarmid, J. Polym. Sci.: Part A: Polymer Chemistry **32**, 2147 (1994).

[13] B. Tareev, *Physics of Dielectric Materials*, Mir Publishers /Moscow (1979).

[14] J. C. Dyre, J. Appl. Phys. **64**, 2456 (1988).

[15] C. O. Yoon, M. Reghu, D. Moses, Y. Cao and A. J. Heeger, Synth. Met. **69**, 255 (1995).

Figure Captions

Figure 1. The nth cell of a typical strip. Here $L = 15$ and we use a gaussian size distribution centered in $l_0 = 6$ and width $\Delta l = 6$. Continuous lines represent the polymer chains (R_c resistors) and broken lines the interchain bridges (RC circuits). The two thick lines are the electrodes.

Figure 2. The longitudinal resistivity $\rho_{//}$ as a function of the frequency f for several values of: (a) doping parameter p_d; (b) intrachain resistance R_c; (c) interchain resistance R_i and fixed capacitance $C = 1\ nF$; (d) concentration k.

Figure 3. Dependence of the real and imaginary parts (ρ' and ρ'' which are represented by thick and thin lines, respectively) of the measured polyaniline resistivity with the frequency f for different temperatures and doping degrees.

Figure 4. Plots of the real and imaginary parts ($\rho'_{//}$ and $\rho''_{//}$) of the simulated longitudinal resistivity (thick and thin lines, respectively) as a function of the frequency f. To reproduce the experimental curves, the interchain resistance R_i should depend on the frequency as shown in the insets. The broken lines corresponds to extrapolated values as explained in the text.

Figure 5. Dyre's hopping resistance $(Re(\frac{1}{\sigma}))$ and the adjusted R_i (inset of Fig. 4a) versus the frequency f. The values of the parameters C, γ_{min} and γ_{max} are $1.0\,10^{10}$, 200 and $1.0\,10^9$.
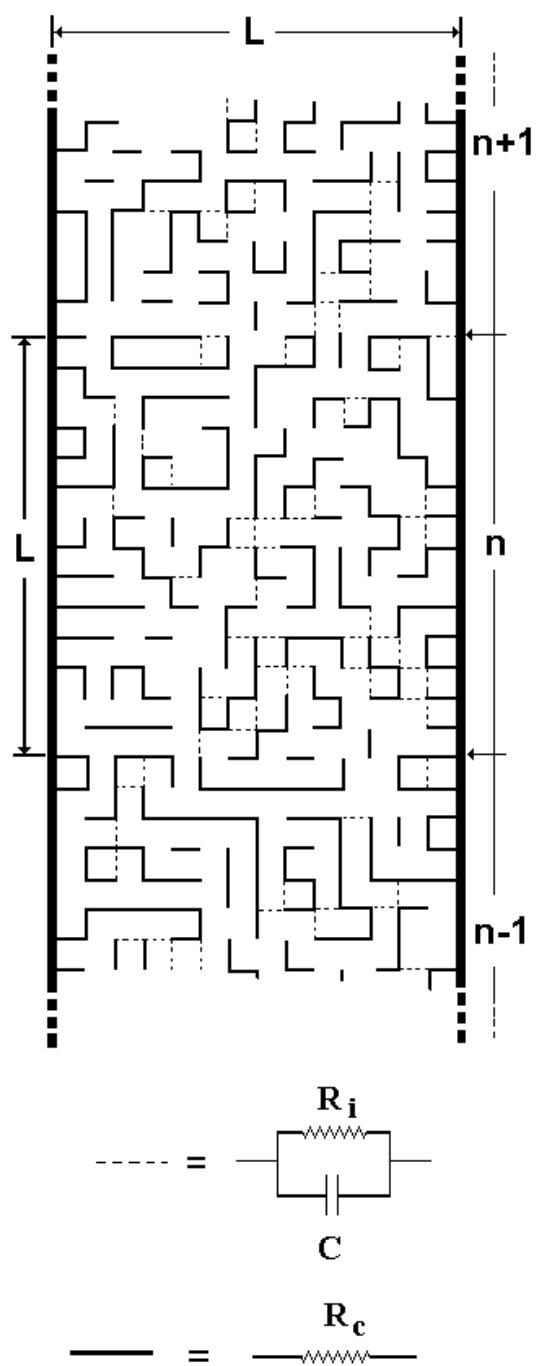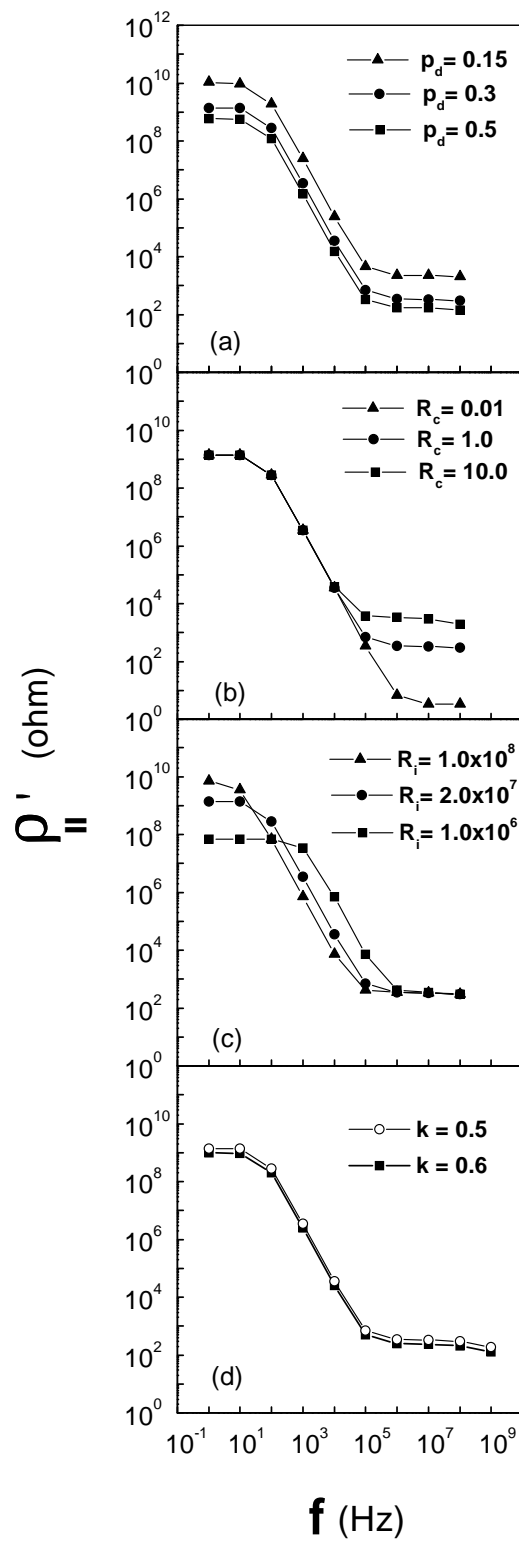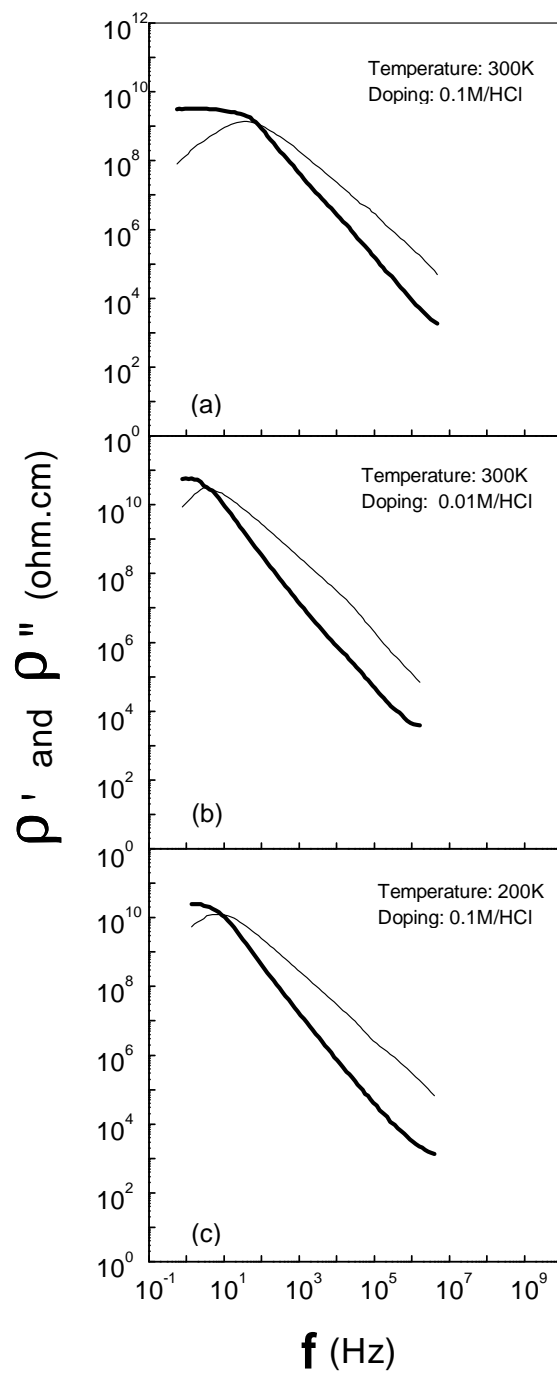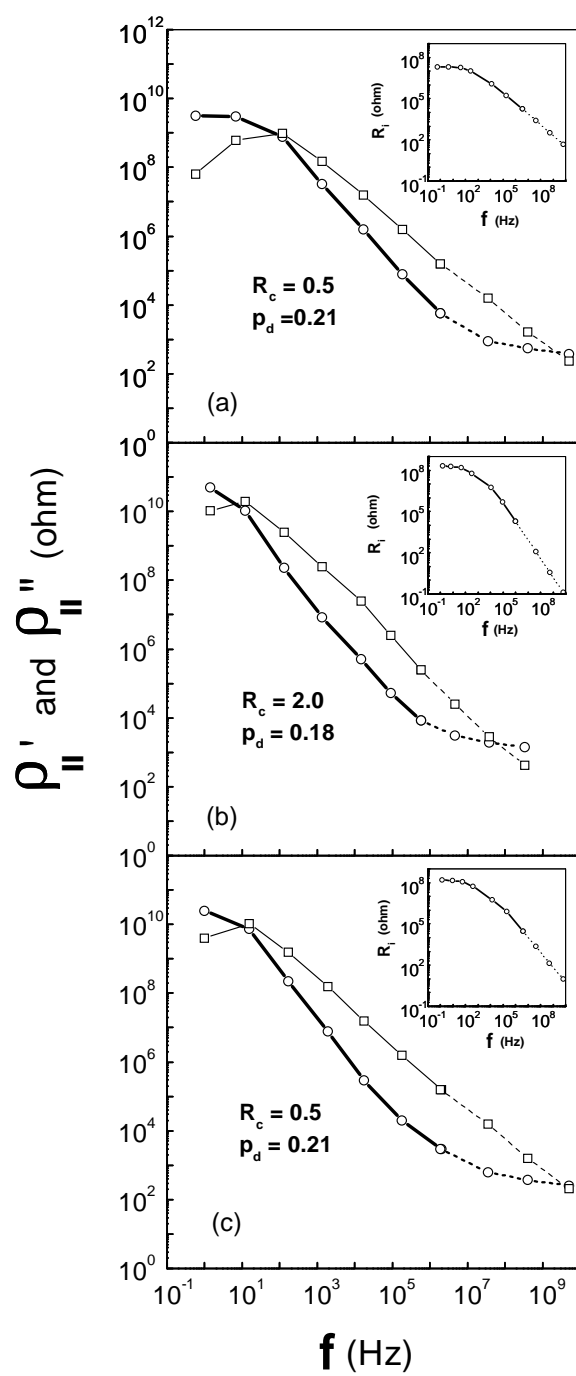
Figure 1

Figure 2

Figure 3

Figure 4

Figure 5